

In: *Estuarine and Coastal Fine Sediment Dynamics - INTERCOH 2003*, Maa, J. P.-Y., L.P. Sanford and D.H. Schoellhamer (eds.), Elsevier, Amsterdam, 321-344.

A preliminary implication of the constant erosion rate model to simulate turbidity maximums in the York River, Virginia, USA

Kwon, J.-I.¹, J.P.-Y. Maa¹ and D.-Y. Lee²

¹Virginia Institute of Marine Science, College of William and Mary, Gloucester Point, VA 23062, USA

²Korea Ocean Research and Development Institute, P.O. Box 29, Ansan, Kyunggi, Korea

KEY WORDS

Suspended sediment transport, model simulation, turbidity maximum, erosion rate.

Numerical simulation of the formation of an Estuarine Turbidity Maximum (ETM) using a constant erosion rate with a stipulated condition that erosion only occurs at tidal accelerating phases was successfully implemented in a three-dimensional hydrodynamic model for the York River. Eight slackwater surveys were carried out during 2001 and 2002 to develop ground truths with measurements at 25 stations along the 120-km York River. Measured salinity and total suspended solid profiles were used to develop “snap shots” for calibration and comparison of results from the numerical simulations. This study indicates that the suggested simple erosion model is capable of simulating suspended sediment transport for addressing the formation of ETM(s). Both the ETM and an occasionally observed secondary turbidity maximum were simulated reasonably well.

1. INTRODUCTION

One of the major difficulties in the simulation of cohesive sediment transport, and thus, the formation of Estuarine Turbidity Maximum (ETM), is to have a simple and reliable erosion process. Currently prevailed erosion models (Parchure and Mehta,

1985; Geyer, 1998; Hayter and Gu, 2001; Lin and Kuo, 2001), either dimensional or non-dimensional, all require at least two or three parameters (details are given in Sec. 3). Based on the conclusions from previous *in-situ* experiments (Maa and Kim, 2002), a single parameter erosion model, *i.e.*, constant erosion rate, was implemented in the three-dimensional (3-D) Hydrodynamic-Eutrophication Model (HEM-3D) to simulate ETMs in the York River (Fig. 1). This approach is a great simplification of erosion process by reducing two or three unknown parameters to a single parameter. Although the current cohesive sediment transport module does not address the flocculation and consolidation processes, it was found that this module works reasonably well for studying the formation of ETM for the two simulated periods in the York River.

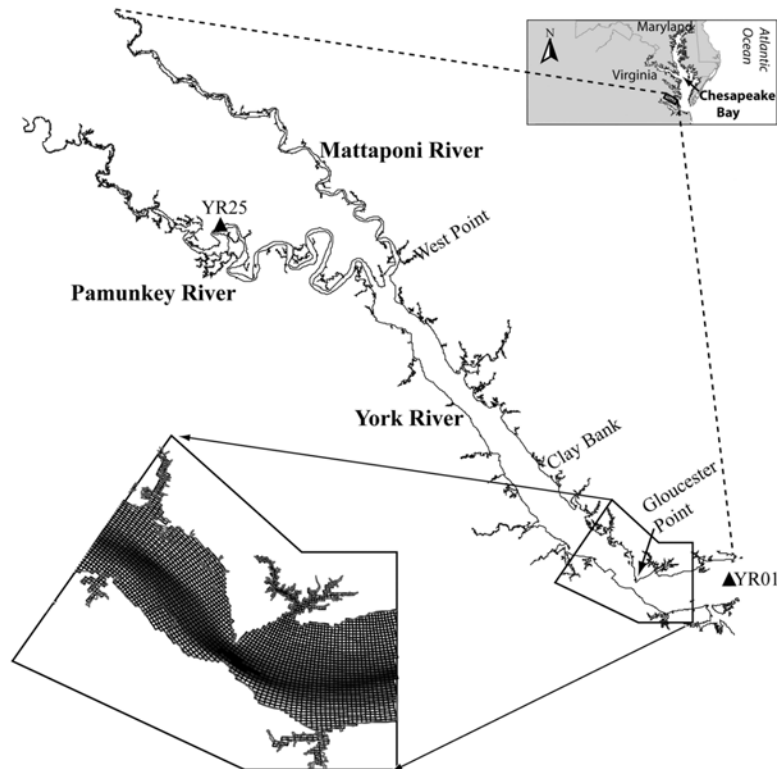


Fig. 1. The York River System, a Subestuary of the Chesapeake Bay. The lower insert shows a part of the curvilinear model grid that follows the bathymetry. Dark area in the lower insert is the channel. Only the 1st (YR01) and the last (YR25) survey stations are shown in the diagram.

The York River system was selected to implement the suspended sediment transport model because of the previous experiences in numerical modeling of hydrodynamic and salinity (Shen *et al.*, 1997), a basic understanding of the suspended sediment distribution (Lin and Kuo, 2001), *in-situ* measurements of erosion rates (Maa and Kim, 2002), and sediment accumulation rates, sediment composition, and bed shear stress measurements (Kim *et al.*, 2000) in this river. Only a small amount of additional fieldwork is required to complete the data sets, greatly facilitating the development of a 3-D suspended sediment transport model.

During 1996 and 1997, a series of slack water surveys (about once a month over one-year period) along the York River was conducted and revealed the general pictures of salinity and sediment distributions in the York River. Two possible ETMs were found. The primary ETM was found near the end of salinity intrusion at the York River, and a secondary ETM was also observed in some of the surveys in the middle of the York River. Using the HEM-3D with the traditional erosion model, Lin and Kuo (2001) revealed a potential mechanism of formation for the secondary ETM (hereafter called STM). However, the Total Suspended Solid (TSS) measurements at only three elevations at each station from that survey are not sufficient for developing a suspended sediment transport model. Thus, a short simulation period, *e.g.*, one or two months, with more TSS profiles in the simulation period would be more reasonable because the dynamics can be closely monitored and simulated.

For the above stated reason, two one-month periods of model simulation were conducted to mimic expected dry (November) and wet (March) seasons. In order to have enough data for calibrating the model, four slackwater surveys were conducted during each period to measure conductivity, temperature and vertical TSS profiles (see Sec. 2 for details).

In order to carry out a good numerical simulation of sediment transport, a basic requirement is enough resolution to address the geometry, especially the channels. Thus, a high-resolution bathymetric grid (grid size about 110 m and 170 m in the cross-channel and along channel directions) was generated. The bottom insert in Fig. 1 shows a part of the grid, near Gloucester Point. Calibration on tidal wave propagation was checked with the M_2 tide (Fig. 2). Also, salt intrusion was successfully simulated for all simulated cases (see Fig. 3 for an example). In general, salinity intrusion simulations indicated that salty water can intrude into the two upstream branches (*i.e.*, Pamunkey and Mattaponi Rivers). Although tidal propagation and salinity intrusion are not the ultimate objectives in this study, they have to be correct in order to have a valid simulation of sediment transport.

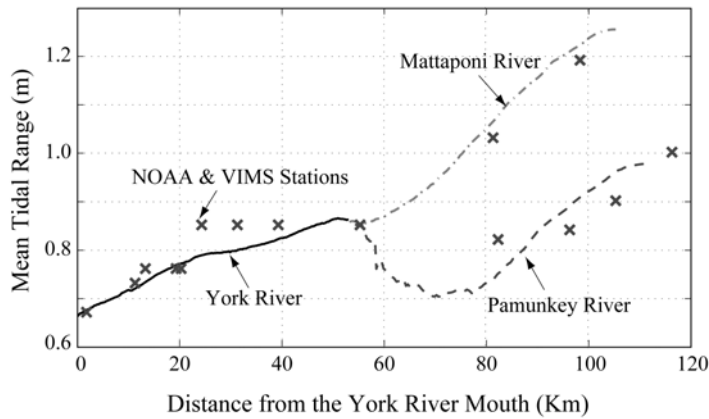


Fig. 2. Comparison of Calculated and Observed (X marks) Mean M_2 Tidal Range Using the New Curvilinear Grid for the Entire York River System.

Field survey results were presented first to show the general features of the suspended sediment distribution in the York River system during the two survey periods in 2001 and 2002. Then, the proposed constant erosion rate model for erosion was explained and implemented with details. The performance of this constant erosion rate model is discussed and suggestions for further improvements are given.

2. RESULTS OF FIELD SURVEYS

Two one-month comprehensive data sets on salinity, temperature, and TSS profiles along the York River system, including tidal freshwater, were collected along 25 stations at slack tide either after a flood or after an ebb. Because of the limited resources and the relatively small dynamic range of freshwater discharge in the Mattaponi River, the slackwater stations on the upstream side were selected along the Pamunkey River.

Freshwater discharge information was obtained from two U. S. Geological Survey (USGS) stations: near Hanover (about 170 km from the York River mouth) on the Pamunkey River and near Beulahville (about 135 km from the York River mouth) on the Mattaponi River. Even though the aim was to cover two different freshwater discharge conditions (wet and dry seasons), the two selected periods of slackwater surveys showed a similar extremely dry condition. These low freshwater discharges caused an

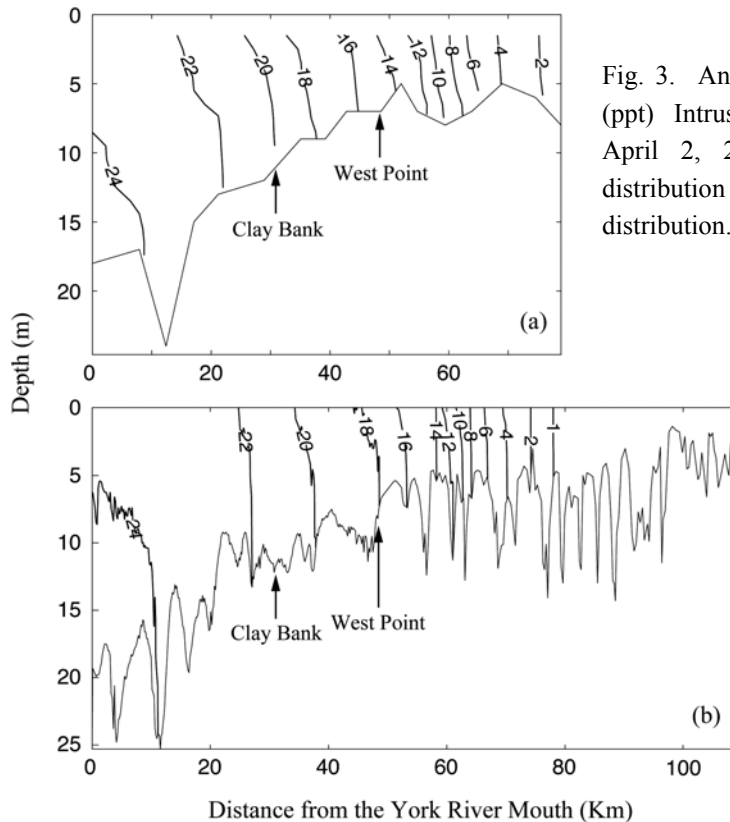


Fig. 3. An Example of Salinity (ppt) Intrusion Simulations on April 2, 2002. (a) Measured distribution and (b) modeled distribution.

abnormal salinity intrusion and a nearly well-mixed salinity distribution at the upstream side of the system (Fig. 3a).

The distance between each slackwater station was short (between 4 to 5 km), because the objective was to obtain a better axial resolution of salinity and TSS gradient at the place where the gradient was large. Not all stations were needed if the axial gradient was small. For this reason, not all surveys had measurements at all 25 stations. Also, some upstream stations were moved a little in each survey to find the maximum TSS profiles. All stations were located in the main channel in order to attain the maximum salinity and TSS information.

Conductivity and temperature profiles were measured using an Apply Micro CTD profiler, model 663. A Seapoint Optical Backscatter Strength (OBS) sensor was

mounted with the CTD profiler to get continuous OBS readings. A water pump with inlet aligned at the same elevation as the OBS was used to take water samples whenever the OBS reading showed a significant change. As a result, water samples were taken at almost all of the surveyed stations to establish an *in-situ* calibration equation for each survey to convert the OBS readings to TSS readings.

All the salinity profiles were reasonably smooth and were used directly to construct the “snap shots” of salinity distribution. The TSS readings, however, required further processing because of many spikes in most of the profiles. Fishes, sea grasses, or any solid subject that moved around the OBS sensor may have caused the abnormal readings. For this reason, it was necessary to remove these spikes and construct smooth TSS profiles.

Not all the TSS profiles showed a high gradient near the bottom. For those stations at the downstream and upstream ends, the TSS profiles were nearly uniform. Only when local convergence was significant, or in the vicinity of ETM, the TSS profiles did have a significant gradient for the lower part of the water column.

All the eight survey results were similar because of the extremely dry year. Nevertheless, the two data sets provided an extreme case for checking the performance of HEM-3D on salinity intrusion, and for validation of TSS distribution on the module developed.

2.1. Salinity distributions

In general, the salinity at the York River mouth was approximately 24-25 ppt. The salinity was still high (*i.e.*, around 15 ppt) at West Point, which is about 50 km upstream from the York River mouth, due to the low freshwater discharge (*e.g.*, Fig. 4).

For a normal hydrological year, the salinity would be about 5 ppt at West Point, and thus, the measured salinity distributions demonstrated a severe dry condition during the two survey periods. The maximum salinity intrusion distance was found to be about 90 km from the York River mouth. The stratification caused by salinity distribution was not strong. For most of the upstream side, the salinity was almost uniform in the vertical direction (Figs. 3a and 4a).

2.2. TSS distributions

On the downstream side of the York River, the TSS profiles clearly indicated a small increase with water depth. Even at depths close to the bottom, the TSS values were small, and only increased about 10 to 20 mg/L. At stations near the upstream turbidity maximum, the TSS profiles increased quickly and had a significant gradient at

the middle water depth. All available TSS profiles for one survey were used to construct a “snap shot” of the TSS distribution for that particular survey.

In general, the TSS concentrations were low and about the same near the York River mouth. The existence of the primary turbidity maximum was obvious and located in the area where the salinity varies from 2 to 10 ppt and the TSS concentration was about 100 - 300 mg/L. A STM was also identified, not always though, near Clay Bank with a much weaker signal (40 - 80 mg/L).

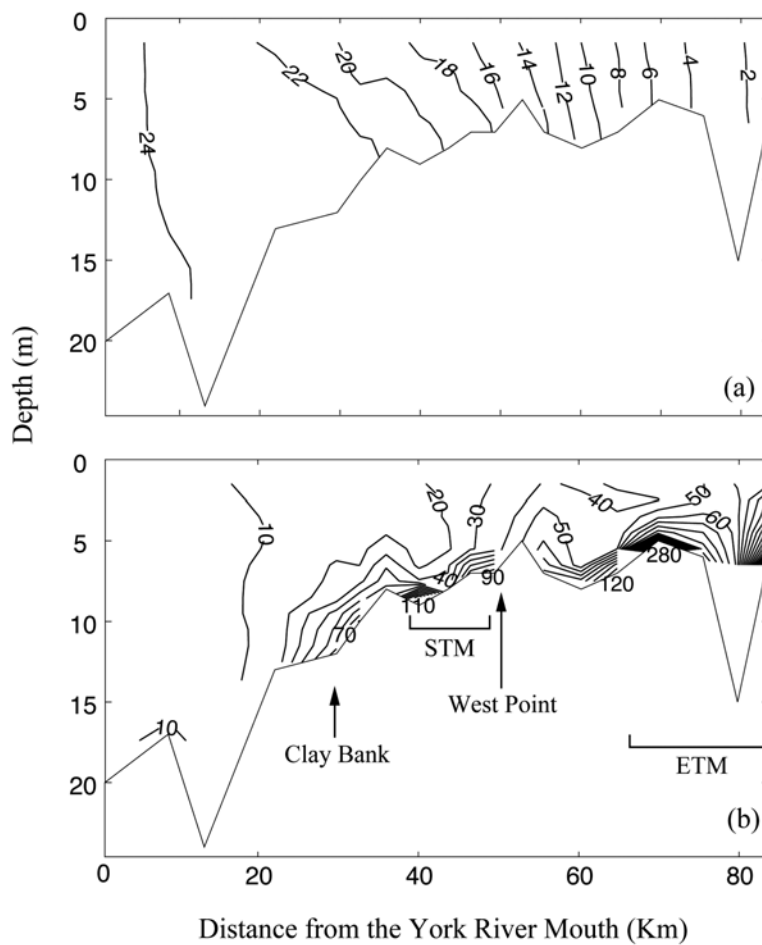


Fig. 4. An Example of Measured (a) Salinity Distribution (ppt) and (b) TSS Distribution (mg/L) on March 19, 2002.

2.3. Downstream boundary conditions

Considering that the near-bottom TSS and salinity information in the deep channel are critical for a better simulation of salinity and TSS distributions and a better understanding of the source for TSS, we selected to extend the monitoring intensity at Station YR01 (Fig. 1) to get the required downstream side boundary conditions.

Every two or three days, salinity and TSS profiles at Station YR01 were measured during the two one-month survey periods. Thus, the TSS and salinity information was available from the channel bottom to the water surface at Station YR01. For other places within this cross section, salinity and TSS profiles were assumed to be the same as those measured at the same elevation in the channel. An example of the salinity boundary condition for the first round of slackwater surveys is summarized in Fig. 5. When using this approach for modeling the TSS and the salinity distributions, amplitudes for salinity and TSS variations should also be measured. Fortunately, these two amplitudes were small, and thus, the impact of using zero amplitude in this study is negligible.

In general, the York River mouth is not a source of TSS because of the measured small TSS values during the two observation periods. The change of salinity and TSS boundary conditions were also limited. The maximum change of salinity was only 4 ppt (*e.g.*, from 24 to 27 ppt in the first survey). Time series of the TSS profiles also indicated that TSS was low (around 10-20 mg/L) and the change of TSS was also small (10-30 mg/L).

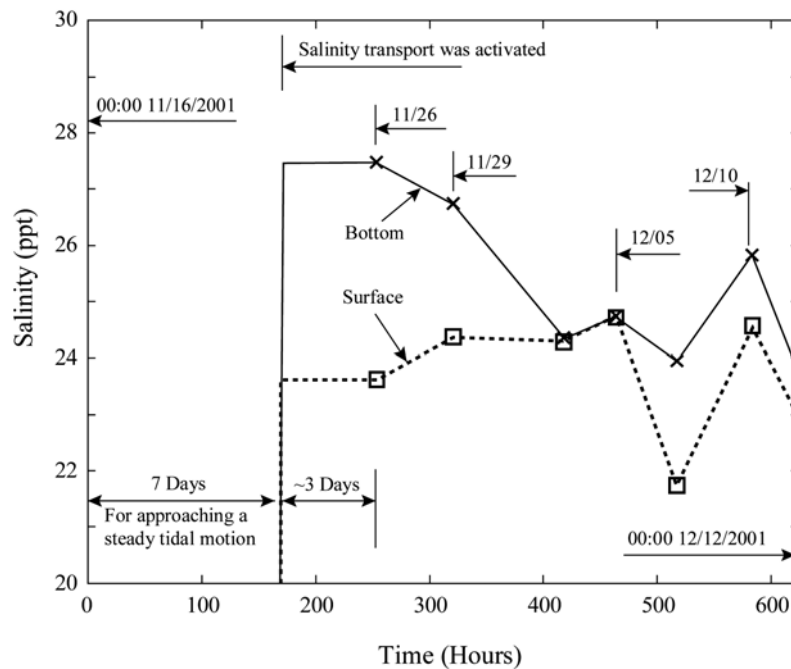


Fig. 5. Salinity Boundary Condition Specified at the York River Mouth for the First set of Slackwater Surveys.

2.4. Upstream boundary conditions

The radiation boundary condition (Chapman, 1985; Hamrick, 1996) was specified at the upstream end to allow tidal waves traveling out of the model domain. Freshwater discharge boundary condition for the modeling periods was obtained from the two USGS stations.

Based on the seven-parameter equation given by Cohn *et al.* (1992), Lin (2001) used 15 years (1979-1994) of data on suspended sediment concentration influx and freshwater discharge at the two USGS stations to work out the “best fit” coefficients for simulated TSS influx to the York River. In this study, the formulation from Lin (2001) was used to calculate TSS concentrations for the two periods of slackwater surveys. Because both periods of slackwater surveys had low freshwater discharge, this implied that the two tributaries did not provide significant sediment sources into the York River, less than 10 mg/L.

2.5. Settling velocity

Turbulence, TSS concentration, and salinity are the major three factors that affect the formation of flocs, and thus, the settling velocity. Turbulence can speed up the formation of flocs (if the turbulence is weak) or break flocs (if the turbulence is strong). TSS concentration indicates the abundance or availability of sediment to form flocs. Salinity allows sediments to form face-to-face flocs by depressing the repulsive electric force on a primary particle’s surface that is much stronger than the attractive force (mainly the Van der Waal’s force). Thus, the floc density in salty water is higher than that in freshwater.

The above statements suggest that the best approach for obtaining the true settling velocity would be to carry out *in-situ* measurements with the above three parameters not affected. In reality, however, a perfect approach for measuring the settling velocity for cohesive sediments does not exist yet. Even the most popular Owen tube method (Owen, 1976) is not perfect, because it blocks out the turbulence. Nevertheless, the Owen tube method was used in this study. Because the Owen tube is not a commercial product, and the limit budget prevented a full scale measurement to address the issue discussed above. Only limited information on settling velocity was obtained.

Surficial sediment collected from the York River at the Clay Bank site was used to estimate the settling velocity (Fig. 6). Because the maximum TSS concentration measured in the York River was about 300 mg/L, there was no need to find a regression equation for the settling velocity of TSS concentration higher than 300 mg/L, at least not for the current modeling effort. Thus, the measured settling velocity can be estimated using the formula

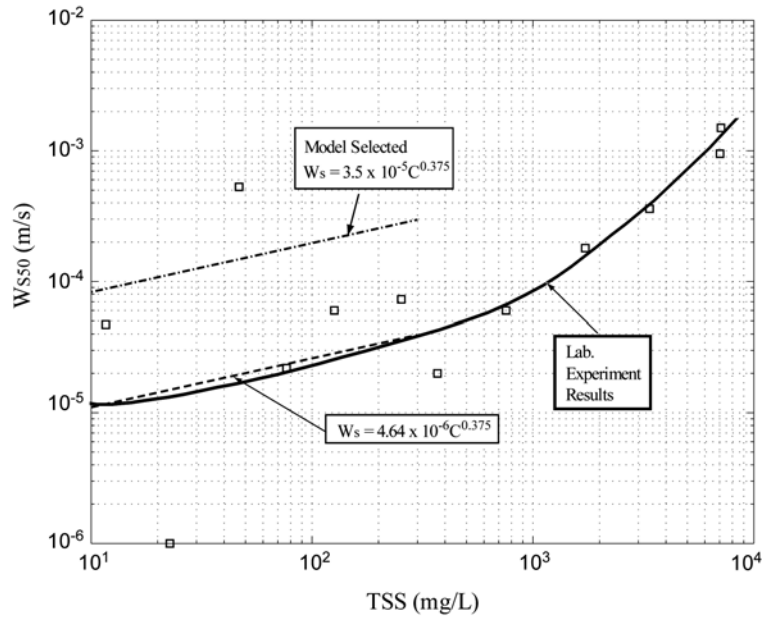


Fig. 6. Measured Settling Velocity for York River Sediments (Clay Bank).

$$w_s = aC^{0.375} \quad (1)$$

where C is the local TSS concentration in mg/L, and a is a constant coefficient equal to 4.64×10^{-6} m/s for freshwater. Equation 1 shows that as the settling velocity increases with the TSS concentration. Because tap water was used in the laboratory experiments, the value of a in Eq. 1 represents a possible low limit. With salinity and turbulence, the value of a should have been higher because of the face-to-face flocculation and a better chance to form flocs. For these reasons, a higher coefficient ($a = 3.5 \times 10^{-5}$ m/s) was used for model simulation.

3. A CONSTANT EROSION RATE MODEL

For sediment transport modeling, the processes that need to be addressed at the bottom boundary include: erosion, deposition, and consolidation. Maa and Kim (2002) used the VIMS Sea Carousel to measure erosion rates at the Clay Bank site in the York

River for four seasons. That is the only site in the York River that directly measurements of erosion rates were made. There is no erosion rate data for other parts of the York River, which spans more than 100 km, nor any data for deposition rate and consolidation rate for this river, therefore it is difficult, if not impossible, to accurately simulate the bottom boundary condition for the entire river.

Simplification of the bottom boundary condition is possible if the river morphology is not the objective (*i.e.*, not considering consolidation), and under this condition, an attempt (with details next) to simulate the formation of ETM was implemented.

3.1. Traditional erosion rate model

Either a dimensional or a non-dimensional excess bed shear stress (Eq. 2) was used to find the erosion rate at a particular time and location, Eq. 2 is hard to use because of the difficulty to know the vertical profile of the critical bed shear stress for erosion, τ_{cr} , at different bed level, z . In Eq. 2, M and n are two constants. Based on an analytical study, Parchure and Mehta (1985) found that n should be $1/2$. For practical applications, however, $n = 1$ is often used for its simplicity (Geyer *et al.*, 1998; Teeter, 2001; Liu *et al.*, 2002; Ganaoui *et al.*, 2004). Even with n specified, Eq. 2 remains impractical because there is no way to know the change of $\tau_{cr}(z)$ with time, especially in the top centimeters of sediment beds because erosion and deposition occur alternatively and frequently. Therefore, an assumption of $\tau_{cr}(z)$ must be frequently made for modeling purposes. This leads to the unavoidable and an impractical tuning of M and $\tau_{cr}(z)$ in the modeling of cohesive sediment transport.

$$\varepsilon = M \left[\frac{\tau_b}{\tau_{cr}(z)} - 1 \right]^n \quad (2)$$

3.2. Simplification of the erosion model

Using the VIMS Sea Carousel for *in-situ* erosion tests (Maa, 1993; Maa *et al.*, 1993; 1998), the observed erosion behavior was always the ‘‘Type 1 behavior’’ (see Eq. 3, Parchure and Mehta, 1985), which means that, for a given bed shear stress (τ_b) that is larger than the τ_{cr} , the eroded sediment mass decreases with time because of the increase of critical bed shear stress $\tau_{cr}(z)$ with depth.

$$\varepsilon(t) = \varepsilon_0 e^{-\lambda t} \quad (3)$$

where ε_0 is the erosion rate at $t = 0$ for the given τ_b , $\varepsilon(t)$ is the erosion rate at a given elapsed time, t , and λ is the rate constant.

In general, the rate constant, $\lambda \approx 0.005 \text{ s}^{-1}$, appears to be a universal constant if the content of sediment has more than 30% of clay. For example, in the clay-rich Baltimore Harbor, Anacostia River near Washington D.C., and San Diego Bay, λ were also around 0.005 s^{-1} (Maa *et al.*, 1998; Maa and Chadwick, this volume). Figure 7a further shows the results of λ for the Clay Bank site in the York River. The physical meaning of $\lambda \approx 0.005 \text{ s}^{-1}$ is that $\varepsilon(t) \approx 0$ in 900 seconds (15 minutes). This is a condition when $\tau_b = \tau_{cr}$. Because tidal flows (*i.e.*, tidal induced τ_b 's) do not change significantly within 20 minutes, tidal erosion is always nearly in equilibrium. In other words, the excess bed shear stress, or the term $[\tau_b/\tau_{cr}(z) - 1]$ is always small during a tidal accelerating phase. During a tidal decelerating phase, however, $[\tau_b/\tau_{cr}(z) - 1]$ is a negative number because $\tau_b < \tau_{cr}$. Therefore, it is reasonable to further simplify Eq. 2 as follows.

$$\begin{aligned} \varepsilon &= \text{constant} && \text{for tidal accelerating phases} \\ \varepsilon &= 0 && \text{for other phases} \end{aligned}$$

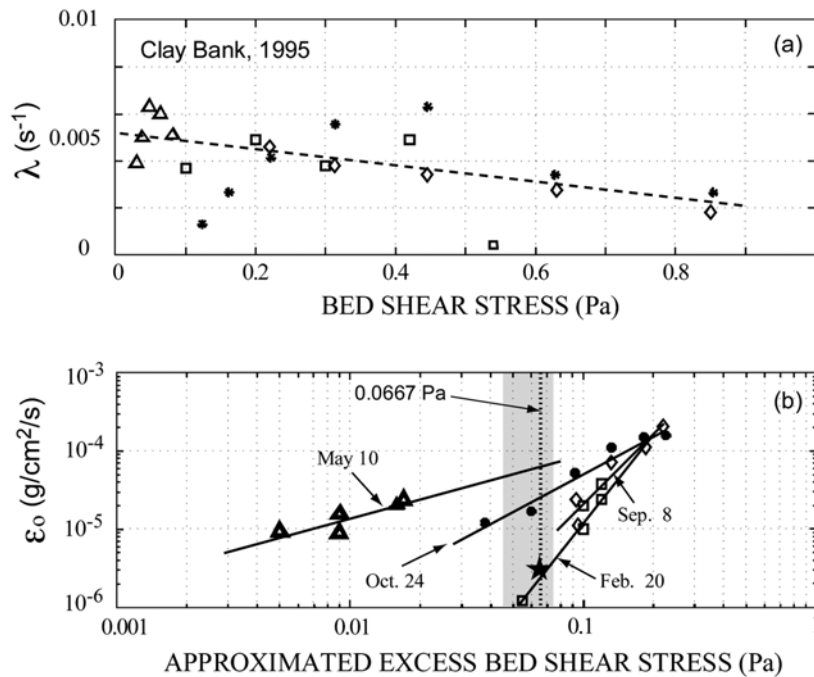


Fig. 7. VIMS Sea Carousel Measured Erosion Rate Constant: (a) λ and (b) ε_0 (after Maa and Kim, 2002)

The simplified bottom boundary condition is also justified from *in-situ* tripod observations of TSS time series at the Clay Bank site (Maa and Kim, 2002). In their study, the near bed (10 cm above bed) TSS concentration always increased during tidal accelerating phases and decreased at other phases. The decrease in TSS during the decelerating phases indicated a drop, if not total stop, of upward diffusion. This implies that erosion ceased, or at least significantly reduced. These features were also observed world-wide (*e.g.*, Sanford and Halka, 1993; Nakagawa, this volume; van den Eynde *et al.*, this volume). The net downward flux would increase the TSS concentration right above the bed, which is far below the lowest sensor. When τ_b was sufficiently small, less than the critical bed shear stress for deposition, τ_{cd} , the near bed suspended sediment deposited and the consolidation process began.

It should be noticed that the duration of erosion between the traditional and current approach is different. The constant erosion rate model begins to resuspend immediately when the flow is accelerating and ceases right after the flow changes into decelerating phase. Compared to the traditional erosion model, the constant erosion rate model starts and stops erosion earlier. This is because the small shear stress at the beginning of a tidal accelerating phase can resuspend the bottom sediment that was deposited during the previous slack period. Also, because the response of sediment erosion is a quick process, the excess bed shear stress become negative when tidal flow decreases. Therefore, erosion stops. The above statements reveal that the difference between the two modules is time. This difference may not affect the formation of ETM.

3.3. Implementation of the constant erosion rate

The maximum bed shear stress induced by tidal currents may vary significantly within an estuary. For this reason, it is not good to use the same constant erosion rate for the entire estuary. Since the information of maximum bed shear stress, $\tau_{bmax}(i,j)$, at all the horizontal water cells (here i and j are cell index numbers) were saved after checking the tidal hydrodynamics and salinity intrusion, it was not difficult to categorize all cells according to their maximum bed shear stress. Thus, the first step was to categorize each cell according to its own τ_{bmax} . Assuming N categories can be established with an equal interval, the constant erosion rate for each cell can be prorated according to a cell's category. It was found that N should be selected at least more than 8 to have enough resolution (see Fig. 8). Notice that in the deep channel at Gloucester Point, between Gloucester Point and West Point, and in the Pamunkey River, the τ_{bmax} was large. On the other hand, τ_{bmax} was small at shallow areas and downstream from Gloucester Point.

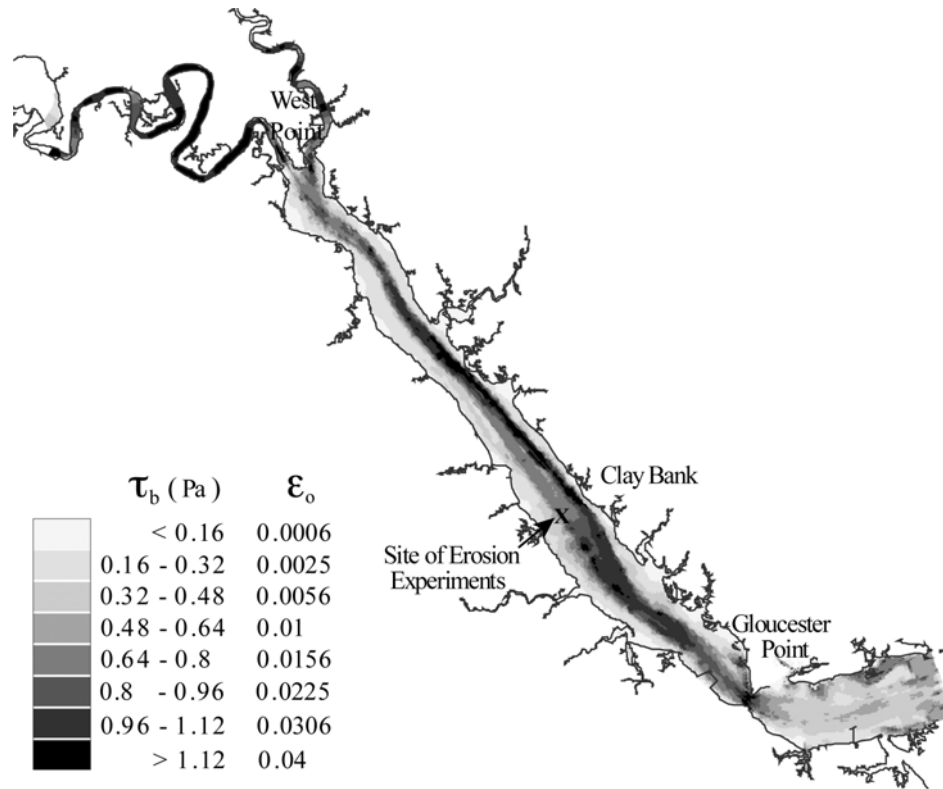


Fig. 8. Distribution of HEM-3D Calculated Maximum Bed Shear Stresses.

The next step was to determine a Reference Constant Erosion Rate (RCER) using *in-situ* measurement results and the τ_{bmax} at the measurement location. The VIMS Sea Carousel erosion experiments were carried out in the secondary channel near Clay Bank (Fig. 8) during 1995. This site had a water depth of 5 m and was located on the south side of the main channel. The maximum bed shear stress at this site was about 0.8 Pa. It was found that the duration of a tidal accelerating phase was about 4 hours at this site (Maa and Kim, 2002), and the maximum bed shear stress must be acquired across this 4 hours. Assuming it increases linearly, the excess bed shear stress can be estimated as $0.8 \text{ Pa} / (240 \text{ min} / 20 \text{ min}) \approx 0.0667 \text{ Pa}$ (dotted line in Fig. 7b). Using this excess bed shear stress, the erosion rate was shown to vary between 0.02 - 0.7 $\text{g/m}^2/\text{s}$. Of course, this is an indication of a significant change with season. Nevertheless, this

procedure provided a base for selecting the RCER. The simulation results given next were based on a selected RCER of $0.0225 \text{ g/m}^2/\text{s}$ (marked as a star in Fig. 7b). This value was chosen because of the extremely dry season that represents no new deposition from upstream discharges for a while.

It is understood that, at those places where τ_{bmax} was larger than 0.8 Pa , the erosion rate should be larger than $0.0225 \text{ g/m}^2/\text{s}$, and similarly, the less the τ_{bmax} , the less the erosion rate. The eight different categories of maximum bed shear stress imply eight different constant erosion rates, and each constant erosion rate is proportional to the rate of $(\tau_{\text{bmax}}/0.8)_c^2$, where c stands for a category and the power of 2 is selected to better fit a non-linear response of erosion rate versus excess bed shear stress (Fig. 7b).

4. RESULTS

One slackwater survey took about one day to finish and was usually started at the York River mouth at a slack tide. After obtaining data at a station, the survey progressed to the next upstream station. The pace of the survey usually matched the tidal propagation, so measurements were always done near slack tide at all the survey stations. Sometimes it was impossible to match with the tide, and a time lag was inevitable. The measured data were used to construct salinity contours and TSS concentration contours given in this paper, and one must know that these are not exactly “snap shots.”

The model calculated results (*i.e.*, water level, current velocity, salinity, TSS, *etc.*), however, are saved for the same time steps for the entire York River system. They are “snap shots.” For this reason, a post-process of model outputs were done to obtain results with times that match with the survey times at each station for comparison. This approach is more accurate when compared with other alternatives such as averaging the results over one tidal cycle. The averaging process in the other approach actually smoothes the output and is hard to compare with the measurements, because they represent two completely different conditions.

In general, the model simulated TSS concentrations in the middle of the water column were slightly higher than observations and the locations of ETM were also off a little, on the order of 5 to 10 km (see Fig. 9 for an example). For further comparing the simulated and the measured surface and bottom TSS concentrations (Fig. 10), an average of 3 m below surface and 1.5 m above the bed were used, respectively.

For Dec. 5, 2001 (Fig. 10a), the simulated ETM was predicted quite well. The near bed TSS concentration matched at about 110 mg/L and the location also matched

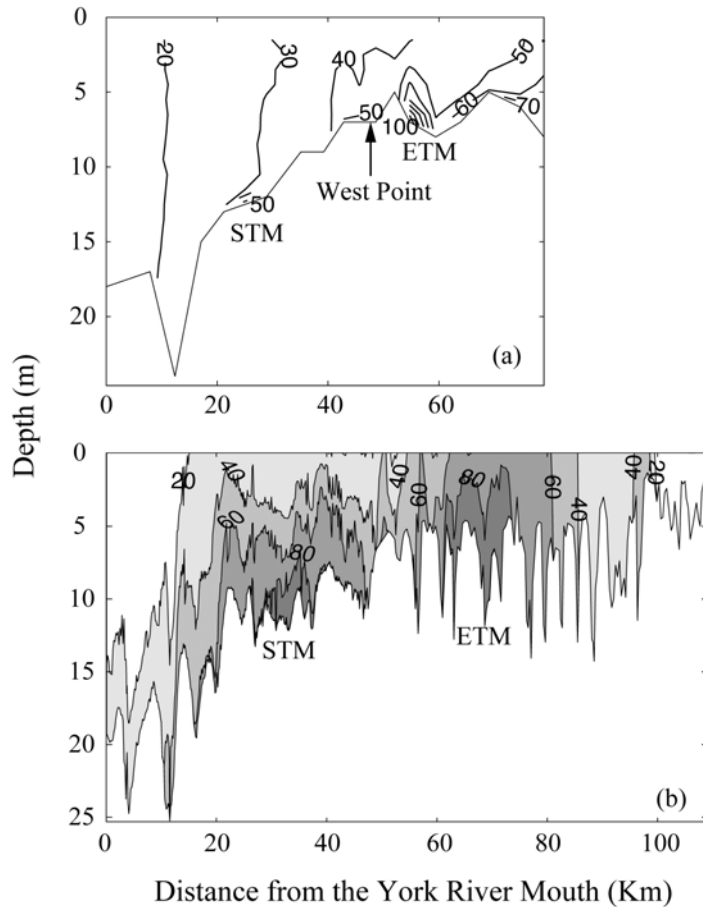


Fig. 9. Comparison of (a) Measured and (b) Modeled TSS Distribution (mg/L) on April 2, 2002.

at about 70 km from the river mouth. But the surface TSS concentration at the ETM site was overestimated. The other peak of measured bottom TSS concentration at 85 km from the mouth may represent a newly developed plume that moved downstream. The location of STM also matched at approximately 30 km from the river mouth, but the simulated TSS concentration was overestimated both at the surface and near the bed.

For April 11, 2002 (Fig. 10b), the center of modeled ETM was off by about 10 km upstream. However, TSS concentrations both at the surface and near the bed were

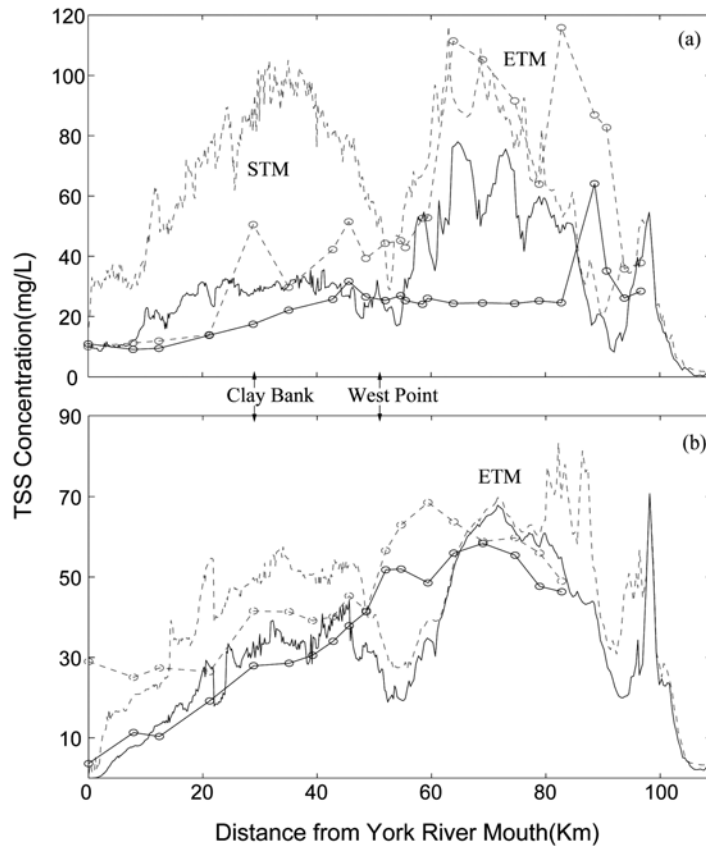


Fig. 10. Comparisons of Observed (lines with circles) and Simulated (lines without circles) TSS Concentrations at two depths. Solid and dashed lines represent surface and bottom TSS Concentrations, respectively. (a) Second Slackwater Survey on Dec. 5, 2001 and (b) Eighth slackwater survey on April 11, 2002.

predicted quite closely compared with measurements. Near Clay Bank, the model predicted a relatively weak STM that was also shown weakly during the survey.

Using the selected approach, a relatively high suspended TSS concentration always showed up at the Clay Bank area, and that may contribute to the existence of the secondary turbidity maximum. Nevertheless, the results presented here indicate that the proposed processes are capable of reproducing the turbidity maximum.

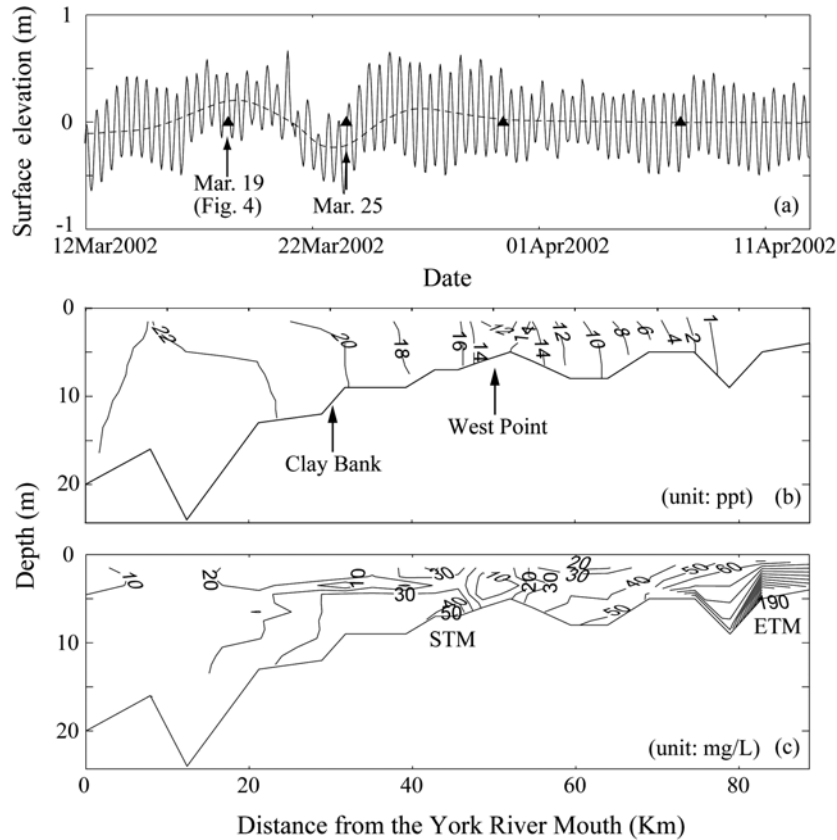


Fig. 11. Effects of a Low-frequency Disturbance on the Relative Location of ETM and Salinity Edge. (a) Time series of surface elevation at Gloucester Point during the second survey: The dashed line is the trend of Mean Water Level and the dates of slackwater surveys are marked with triangles. (b) The salinity distribution on March 25, 2002 (the second triangle on (a)) and (c) the TSS concentration distribution at the same time.

During the eight slackwater surveys, the ETM was always established on the downstream side of the head of salt intrusion (see Fig. 4, for example) except one case given in Fig. 11. Because all surveys were conducted in the low river discharge periods, salt intrusion distances were quite long and the ETMs were formed at a far upstream direction, but lags behind the head of the salt intrusion. The relationship between the head of salt intrusion and ETM was discussed by many other researchers (Geyer, 1993; Uncles *et al.*, 1993; Lin, 2001). It is a complicated process interacted

with several factors (*e.g.*, tide, TSS concentration, estuarine circulation, and stratification). However, in this study another possible factor was observed. Between March 19 and March 25, 2002, there was a set down of the mean water level (Fig. 11a). Due to this set down, the head of salt intrusion (2 ppt) moved about 5 km downstream (see Fig. 4a and Fig. 11b). This is because the increase in pressure gradient produced more downstream-flux from Pamunkey River. But the ETM did not adjust immediately to the change of this hydrodynamic condition. Also, at the upstream side of West Point a relatively less saline and TSS concentration mass pocket was observed. Unfortunately there is not sufficient data to verify where this plume originated. It might have come to York River from the Mattaponi River during an ebb, and when the tide changed to flood, a part of the plume flowed into the Pamunkey River. Although in general, the freshwater discharge from the Mattaponi River is only half of the Pamunkey River, but the time to reach the York River may vary with the local rain events that there is not enough data for studying at this time. Regardless of this plume's origin, it might alter the movement of salt and sediment (see 6-14 isohalines in Fig. 11b). Notice that the freshwater discharge from the Pamunkey River also doubled from 5 to 10 m³/s during this set down event. This increase of freshwater discharge may enhance the stratification somehow, and thus, may affect both the locations of the head of salt intrusion and the ETM. A further study is required to better understand the relationship between the head of salt intrusion and the location of the ETM in the York River system.

5. DISCUSSION

To simulate sediment transport is not a simple task, because the simulation of tidal hydrodynamics must be right (including tidal range, tidal phase, and salinity intrusion). With the new high resolution bathymetric grid, the above mentioned processes were all successfully simulated using the HEM-3D model.

One of the difficulties faced in this study was how to set a constant erosion rate for each bed cell, because there was only one *in-situ* measurement (near Clay Bank) in the York River. The method presented in this study with 8 categories of maximum bed shear stress is simple but arbitrary. It is possible to extend this approach by using the rate of the maximum bed shear stresses, $[\tau_{bmax}(i,j)*RCER / \tau_{Rbmax}]^k$, directly. Where τ_{Rbmax} is the maximum bed shear stress at the reference site. The use of $k = 2$ is arbitrary and may require more study to better describe the observed large range of erosion rate.

Even though the constant erosion rate gives a simple way to successfully address the erosion process, it should be noticed that both periods of simulation were under extremely dry condition. Considering various hydrodynamic and sediment bed conditions, the suggested “constant erosion rate model” must be able to reflect the change of these conditions. For example, it is shown clearly in Fig. 7b that the constant erosion rate could vary significantly for a given excess bed shear stress, depending on the condition of the sediment bed and hydrodynamic conditions.

Inasmuch as the excess bed shear stress depends on the applied bed shear stress caused by the hydrodynamic forces and the critical bed shear stress for erosion controlled by sediments, the change of the constant erosion rate must reflect the possible change of hydrodynamics and sediment conditions in time and space. In this study the excess bed shear stress was calculated using the maximum bed shear stress from the model simulation with only M_2 tide and one bed condition. The possible changes on τ_{cr} for different beds and the change of τ_b due to flood-ebb variation and spring-neap tides variation were not included. Even with these limitations, the proposed constant erosion rate model works reasonable well because the M_2 tide is the dominant tide in the York River. It represents 89% of the total tidal energy (Sisson *et al.*, 1997). Thus, the true maximum bed shear stress and duration of accelerating phases only vary slightly for the true conditions simulated. To make a constant erosion rate more precise, the true maximum bed shear stress and the duration of accelerating phase should be found first with all the tidal components for a long enough period to cover spring-neap cycles. Thus, even for a fixed τ_{cr} , the excess bed shear stress, τ_{ex} , should have a range (see the gray area in Fig. 7b), not a single value. This will further complicate the modeling effort, and more study is necessary to fully address the need/justification of this modification.

It should be noticed that a more important factor, the bed condition, *i.e.*, τ_{cr} , should have a dominant influence on erosion. The bed conditions may also change with time, especially when there are new sediment coming with storm freshwater discharges. For example, the high erosion rate for May 10th shown in Fig. 7b was caused by a significant storm event eight days before the date of the erosion test. Therefore, newly deposited materials were relatively abundant at that time at Clay Bank (Maa and Kim, 2002). With time, the consolidation process gradually changes the easily erodible sediment into ordinary sediment, and the erosion rate also decreases back to normal conditions. Since the new sediment input from the upstream side is proportional to the freshwater discharge, it is possible to assume that the change of the erosion rate is also proportional to the freshwater discharge. Thus, a constant erosion rate can be tuned with the freshwater discharge to reflect the change of bed materials. However, there

should be a time delay in this process for each section of a long river. So far, the modification of the constant erosion rate at the reference site due to the change of freshwater discharge is explained. However, the freshwater discharge may also have an effect on the spatial variability. The clear spatial variability in Baltimore Harbor (Maa *et al.*, 1998) was reported, although it was not caused by the freshwater discharge. To consider the spatial variability of the erosion rate, an additional function (varies with distance) can be used to modify the constant erosion rate model. More studies are needed to find the system response that best describes the above process. By combining the above three adjustments, it is feasible to obtain better modeling capability for suspended sediment transport.

6. CONCLUSIONS

(1) A total of eight field surveys on the salinity and total suspended sediment (TSS) profiles along the York River were conducted during two one-month periods (Nov.-Dec., 2001 and March-April, 2002). Because of the unexpected extremely dry seasons during those periods, the survey results in terms of salinity and TSS distributions were very close. There were no significant sediment inputs from both land and ocean. Therefore, sediment eroded from the bed within the York River system must be the source.

(2) The survey results showed that the estuarine turbidity maximum (ETM) was abnormally located about 30 km upstream from West Point. For a normal hydrological year, the ETM was usually located on the downstream side of West Point. A Secondary Turbidity Maximum (STM) was also identified in the York River with a much weaker signal.

(3) A new curvilinear orthogonal bathymetric grid for the York River system was developed to clearly represent all the navigation channels. Model performances on tidal propagation and salinity intrusion were excellent using this new grid.

(4) A series of experiments on the settling velocity of York River sediment indicated that the settling velocity was affected by the concentration of TSS that proved the importance of sediment availability. The influences of salinity and turbulence on the settling velocity remain unaddressed. The limited numerical experiment showed that a higher settling velocity should be used in the modeling of TSS distribution.

(5) Using a simple model for erosion, *i.e.*, erosion occurs only when the tidal flow is in accelerating phases, and during this period of time, a constant erosion rate (which was determined based on the local maximum bed shear stress and results from previous

erosion tests) was successfully used to simulate suspended sediment transport for the York River system.

(6) Further improvements on the constant erosion rate model are necessary to address the temporal and spatial variation of this “constant erosion rate” approach to reflect the seasonal change on the bed condition, as well as the different hydrodynamic conditions. Freshwater discharge is likely the most important parameter to alter the bed condition (*i.e.*, critical bed shear stress for erosion).

ACKNOWLEDGMENTS

Special thanks to Mr. S. Wilson, W. Reisner, R. Gammisch, and H.-K. Ha for their help on field work. Thanks also go to Mr. M. Sisson and Drs. S.-C. Kim and J. Shen for their support and encouragement. The support from the Chesapeake Bay Program FY2001, Environmental Protection Agency under contract number CB-983431-01-0 is also acknowledged. This is a contribution of the Virginia Institute of Marine Science (2648).

REFERENCES

- Chapman, D.C. 1985. Numerical treatment of cross-shelf open boundaries in a barotropic coastal ocean model. *Journal of Physical Oceanography*, 15, 1060-1075.
- Cohn, T.A., D.L. Caulder, E.J. Gilroy, L.D. Zynjuk and R.M. Summers. 1992. The validity of a simple statistical model for estimating fluvial constituent loads: An empirical study involving nutrient loads entering Chesapeake Bay. *Water Resources Research*, 28(9), 2353-2363.
- Ganaoui, O.E., E. Schaaff, P. Boyer, M. Amielh, F. Anselmet and C. Grenz. 2004. The deposition and erosion of cohesive sediments determined by a multi-class model. *Estuarine, Coastal and Shelf Science*, 60, 457-475.
- Geyer, W.R., 1993. The importance of suppression of turbulence by stratification on the estuarine turbidity maximum. *Estuaries*, 16(1), 113-125.
- Geyer, W.R, R.P. Signell and G.C. Kineke. 1998. Lateral trapping of sediment in a partially mixed estuary. In: *Physics of Estuaries and Coastal Seas*. Dronkers, J. and M. Scheffers (eds.), A.A. Balkema, Rotterdam, 115-124.

- Hamrick, J.M. 1996. *Users manual for the environmental fluid dynamics code*. Special report No. 331 in Applied Marine Science and Ocean Engineering, Virginia Institute of Marine Science, College of William and Mary, Gloucester Point, 159p.
- Hayter, E.J. and R. Gu. 2001. Prediction of contaminated sediment transport in the Maurice River-Union Lake, New Jersey, USA. In: *Coastal and Estuarine Fine Sediment Processes*. McAnally, W. H. and A. J. Metha (eds.), Elsevier, Amsterdam, 439-458.
- Kim, S.C., C. Friedrichs, J.P.-Y. Maa and L.D. Wright. 2000. Estimating bottom stress in a tidal boundary layer from acoustic doppler velocimeter data. *Journal of Hydraulic Engineering*, 126(6), 399-406.
- Lin, J. 2001. *A study of the secondary turbidity maximum in the York River Estuary, Virginia*. Ph.D Dissertation, College of William and Mary, Williamsburg, VA.
- Lin, J. and A.Y. Kuo. 2001. Secondary turbidity maximum in a partially mixed microtidal estuary. *Estuaries*, 24(5), 707-720.
- Liu, W.-C., M.-H. Hsu and A.Y. Kuo. 2002. Modelling of hydrodynamics and cohesive sediment transport in Tanshui River estuarine system, Taiwan. *Marine Pollution Bulletin*, 44,1076-1088.
- Maa, J.P.-Y. and B. Chadwick. This volume. Estimation of annual averaged propeller erosion rate in San Diego Bay, California. In: *Coastal and Estuarine Fine Sediment Processes*. Maa, P.-Y., L.P. Sanford and D.H. Schoellhamer (eds.), Elsevier, Amsterdam, this volume.
- Maa, J.P.-Y. and S.-C. Kim. 2002. A constant erosion rate model for fine sediment in the York River, Virginia. *Environmental Fluid Mechanics*, 1, 343-360.
- Maa, J.P.-Y., L.P. Sanford and J.P. Halka. 1998. Sediment resuspension characteristics in the Baltimore harbor. *Marine Geology*, 146, 137-145.
- Maa, J.P.-Y. 1993. VIMS Sea Carousel: Its hydrodynamic characteristics. In: *Near-shore and Estuarine Cohesive Sediment Transport*. Mehta, A.J. (ed.), American Geophysical Union, Washington, D.C., 265-280.
- Maa, J.P.-Y., L.D. Wright, C.-H. Lee and T.W. Shannon. 1993. VIMS Sea Carousel: A field instrument for studying sediment transport. *Marine Geology*, 115, 271-287.
- Nakagawa, Y. This volume. Fine sediment transport in Ariake Bay, Japan. In: *Coastal and Estuarine Fine Sediment Processes*. Maa, P.-Y., L.P. Sanford, and D.H. Schoellhamer (eds.), Elsevier, Amsterdam, this volume.
- Owen, M.W. 1976. *Determination of the settling velocities of cohesive muds*. Report Number IT 161, Hydraulics Research Station, Wallingford, Oxon.
- Parchure, T.M. and A.J. Mehta. 1985. Erosion of soft cohesive sediment deposits. *Journal of Hydraulic Engineering*, ASCE, 111(10), 1308-1326.

- Sanford, L.P. and J.P. Halka. 1993. Assessing the paradigm of mutually exclusive erosion and deposition of mud, with examples from upper Chesapeake Bay. *Marine Geology*, 114, 37-57.
- Sisson, G.M., J. Shen, S.-C. Kim, J.D. Boon and A.Y. Kuo. 1997. *VIMS 3-D Hydrodynamic Eutrophication Model (HEM-3D): Application of the hydrodynamic model to the York River system*. Special report in Applied Marine Science and Ocean Engineering, No. 341, Virginia Institute of Marine Science, College of William and Mary, Gloucester Point.
- Shen, J., M. Sisson, A.Y. Kuo, J.D. Boon and S. Kim. 1997. Three-dimensional numerical modeling of the tidal York River system, Virginia. *Proceedings of the 5th International Conference on Estuarine and Coastal Modeling*, ASCE, Reston, 495-510.
- Teeter, A.M. 2001. Clay-silt sediment modeling using multiple grain classes. Part II: Application to shallow-water resuspension and deposition. In: *Coastal and Estuarine Fine Sediment Processes*. McAnally, W.H and A.J. Metha (eds.), Elsevier, Amsterdam, 173-187.
- Van den Eynde, P., B. Nechad, M. Fettweis and F. Francken. This volume. Seasonal variability of suspended particulate matter observed from SeaWiFS images near the Belgian coast. In: *Coastal and Estuarine Fine Sediment Processes*. Maa, J.P.-Y., L.P. Sanford and D.H. Schoellhamer (eds.), Elsevier, Amsterdam, this volume.
- Uncles, R.J. and J.A. Stephens. 1993. The freshwater-saltwater interface and its relationship to the turbidity maximum in the Tamar Estuary, United Kingdom. *Estuaries*, 16(1), 126-141.